Shock compression and brightness temperature of a shock wave front in argon. Electron screening of radiation

F. V. Grigor'ev, S. B. Kormer, O. L. Mikhaĭlova, M. A. Mochalov, and V. D. Urlin

(Submitted 26 July 1984)
Zh. Eksp. Teor. Fiz. **88**, 1271–1280 (April 1985)

An experimental investigation was made of argon in the density range $\rho = 2.6$–3.6 g/cm^3 at pressures $P = 140$–670 kbar under conditions of shock compression from an initial state characterized by $\rho_0 = 1.4$ g/cm^3 and $T_0 = 87$ K. An optical method was used to determine the brightness temperature between 3700 and 17 000 K. The equations of state of argon in the solid and liquid phases were determined. The calculated and experimental shock adiabats and melting curves were compared. The temperature was calculated from the equation of state allowing for the influence of thermal excitation of electrons from the valence to the conduction band. The measured brightness temperature of argon was found to lag behind that calculated from the equation of state on the basis of a theory which allows for the kinetics of the process of establishment of a thermodynamic equilibrium between electrons and the lattice.

INTRODUCTION

Compression of argon to high pressures produces a structure which is the most tightly packed configuration in the condensed state so that structural phase transitions cannot be expected. Therefore, the equation of state of compressed argon should be similar to the already investigated equations of state of close-packed metals[1–3] or of condensed molecular hydrogen.[4]

We shall report the experimental results on shock compression of liquid argon up to 670 kbar beginning from an initial state characterized by $\rho_0 = 1.4$ g/cm^3, $T_0 = 87$ K and also measurements of the brightness temperature in the range from 3700 to 17 000 K for argon subjected to shock compression.

A method tested in Refs. 1–4 was used to find the equation of state for solid and liquid argon and to compare it with the available experimental data: in the solid phase—with the isotherms at $T = 0$ and 77 K (Ref. 5), as well as with experiments on shock compression of solid argon[6,7]; in the liquid phase—with the experimental data on single and double shock compression.[8–10] The calculated melting curve was compared with the experimental dependences given in Refs. 7–14.

We found that the form of the shock adiabat began to manifest the influence of thermal excitation of electrons from the valence to the conduction band at pressures $P > 300$ kbar. Shock adiabats calculated allowing for the thermal excitation of electrons are in full agreement with the experimental data on the shock compression of argon obtained in the present study and from Refs. 8 and 9.

The experimental determination of the brightness temperature made it possible to check independently the correctness of the definition of the parameters of the equation of state or argon, particularly its specific heat. Moreover, the results gave information on the shock wave front structure in a condensed sample and on the kinetics of heating of electrons in the conduction band.

EXPERIMENTAL RESULTS

Liquid argon was subjected to shock compression from an initial state characterized by $\rho_0 = 1.4$ g/cm^3 and $T_0 = 87$ K until a density of 3.6 g/cm^3 was reached at a pressure of 670 kbar.

The construction of a system for the determination of the shock-wave velocity and of the brightness temperature of liquid argon is shown in Fig. 1. Argon was poured into the inner cavity of a chamber and the space surrounding it was evacuated.

The shock wave velocity was measured by an electric-contact method.[15] Boiling of argon in the cavities where the contacts were located ceased after a few minutes and did not start again throughout the rest of the experiment. A shock wave was created in liquid argon by explosive systems similar to those described in Refs. 2, 16, and 17; the parameters of these systems are listed in Table I. The screens through which a shock wave was applied to liquid argon were plates made of Al, Cu, or Fe for which the shock adiabats were known.[17–19]

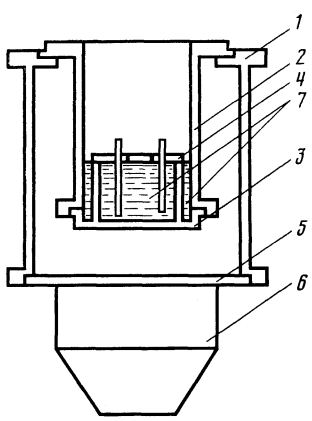

FIG. 1. Construction of an experimental system: 1) casing; 2) chamber; 3) screen; 4) plate with contacts; 5) striker; 6) explosive charge; 7) liquid argon.

 0038-5646/85/040751-07$04.00

TABLE I.

System No.	Screen material	Parameters of shock waves in screens		Parameters of Hugoniot adiabat of liquid argon ($\rho_0 = 1.4$ g/cm^3)				
		u, km/sec	P, kbar	u, km/sec	D, km/sec	P, kbar	ρ, g/cm^3	$T\cdot10^{-3}$, K
1	Al	1,50	298	2,19	4,68±0,02	143±1	2,63±0,01	3,7±0,2
2	Cu	1,63	924	2,71	5,60±0,06	210±3	2,71±0,03	5,7±0,2
3	Cu	1,75	1020	2,9	5,90±0,03	240±2	2,75±0,02	7,1±0,2
4	Al	2,51	594	3,43	6,65±0,03	320±3	2,89±0,02	9,3±0,4
5	Al	2,72	666	3,66	7,02±0,04	360±3	2,93±0,02	11±0,6
6	Fe	2,48	1536	3,98	7,42±0,08	410±5	3,02±0,04	12,4±0,8
7	Al	3,32	886	4,39	7,94±0,09	490±11	3,13±0,08	13,9±0,9
8	Al	3,65	1017	4,90	8,44±0,12	580±13	3,34±0,10	15,6±1,1
9	Fe	3,05	2109	5,42	8,84±0,11	670±15	3,62±0,12	16,8±1,2

The shock wave velocity D in liquid argon was determined by the reflection method[20] and then used to find the mass velocity u of matter behind the shock wave front and the pressure P in the shock-compressed matter. An allowance was made for cooling of the screen material to $T = 87$ K. Between five and eight independent experiments were carried out using each system. The shock wave velocity was found in each experiment employing four or five pairs of contacts on a base about 3 mm long. The rms error in the shock wave velocity measurements did not exceed 1.5%. The experimental results are listed in Table I. Measurements were made also of the parameters of a shock wave in argon reflected from an Al plate when compression was due to two shock waves. The results obtained were as follows: $u_2 = 1.93 \pm 0.07$ km/sec, $\rho_2 = 3.31 \pm 0.11$ g/cm^3, $P_2 = 420 \pm 20$ kbar, in good agreement with the results reported in Ref. 10 (see Fig. 5 below). The parameters of the first shock wave are listed in Table I (system No. 3).

The brightness measurements of shock-compressed liquid argon were determined by a photographic method similar to that described in Ref. 21; this was done in the red part of the spectrum ($\lambda_{\text{eff}} = 0.67\,\mu$). The radiation emitted by the shock wave front was recorded employing an SFR-2M image converter camera on a photographic film placed behind a KS-14 red light filter. The combination of the spectra transmission of this filter and the spectral sensitivity of the photographic film selected a spectral interval $\Delta\lambda = 40$ nm wide at half-amplitude. The measurements were made on a comparison principle using an IKF-50 xenon lamp with a brightness temperature of 6800 K (see Ref. 22) as the source of standard radiation. The characteristic curve of the photograpic film was recorded by placing a nine-stage platinum attenuator in the focal arc of the SFR-2M image converter camera. The position of the attenuator was selected so that it was located within a region of constant intensity of the standard radiation. A typical densitogram of the radiation from the shock wave front in liquid nitrogen is shown in Fig. 2. The experimental results were analyzed by the method of actinic fluxes[23] and are listed in Table I. The rms error in the average value of the temperature was calculated from measurements made in five to eight independent experiments (Table I). A steep rise of the brightness of the radiation of the front to its maximum value (which occurred in a rise time $\tau_r \sim 0.1$–0.2 μsec) was evidence of a large value of the absorption coefficient. Moreover, as pointed out in Ref. 24, the reflection coefficient of the shock wave front was low ($\leqslant 2\%$) for a large class of transparent insulators. Therefore, the transparency and the reflectivity of the shock wave front in liquid argon could be ignored in the temperature measurements.

We assumed that the fall of the brightness of the radiation emitted by the front in the time interval $t > \tau^*$ (Fig. 2) was due to the shock wave catching up with an unloading wave from a striker and in this way we found the velocity of sound for the state of argon with $\rho = 2.75$ g/cm^3 and $P = 240$ kbar. The velocity $C = 5.37$ km/sec found in this way was in good agreement with the value $C = 5.3$ km/sec calculated from the equation of state derived as described below.

EQUATION OF STATE OF ARGON IN SOLID AND LIQUID PHASES

The form of the equation of state of argon in solid and liquid phases was assumed to be similar to that used in Refs. 3 and 4. In the case of argon it was possible to ignore the contribution of zero-point vibrations to the pressure and energy.

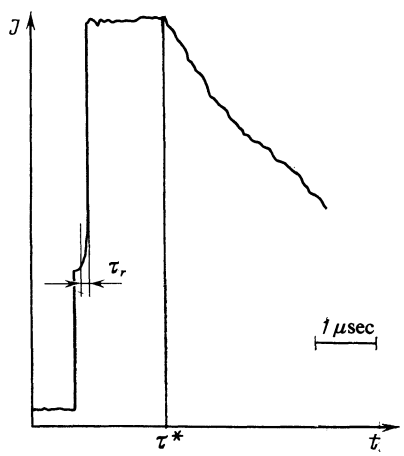

FIG. 2. Typical densitogram of the radiation emitted by shock-compressed argon: τ_r is the rise time of the brightness of the radiation of the shock wave front to its maximum value; τ^* is the time of arrival of an unloading wave.

The free energy of the solid and liquid phases of argon is described by

$$F_S = E_x + RT[3\ln(1-e^{-\Theta/T}) - D(\Theta/T)], \quad (1)$$

$$F_L = E_x + 3RT\{\ln[(\Theta/T)(1+Z)^{1/3}] - b\} + 3RT_0 f. \quad (2)$$

The curve for the elastic interaction of atoms is approximated in these equations by a dependence of the type[25]

$$E_x = \frac{3}{\rho_k}\sum_{i=1}\frac{a_i}{i}(\delta^{i/3}-1), \quad (3)$$

where $\delta = \rho/\rho_0$; ρ_0 is the density at $P = 0$ and $T = 0$; a_i are empirical constants.

The relationship between the Debye temperature Θ and the density in the Debye function is

$$\Theta = \frac{\Theta_0}{C_x(\delta=1)}\delta^{1/3}\left(C_x^2 - n\frac{2P_x}{3\rho}\right)^{1/3}, \quad (4)$$

where $C_x^2 = dP_x/d\rho$ and $P_x = \rho^2 dE_x/d\rho$.

In Eq. (2) the parameters

$$Z = lRT\left(C_x^2 - n\frac{2P_x}{3\rho}\right)^{-1}, \quad f = c + \frac{a}{r}\left[\left(\frac{\delta}{\delta_0}\right)^r - 1\right] \quad (5)$$

determine the degree of deviation of the thermal and elastic properties of the liquid from those of the solid phase.

The notation used in Eqs. (1)–(5) is as follows: R is the gas constant; δ_0 and T_0 are the relative density and temperature at the melting point at atmospheric pressure; n, a, b, c, l, r are empirical constants.

The justification for the selected form of the equation of state and the methods for finding its parameters are given in Refs. 1–4. The parameters of the equation of state in the solid and liquid phases were determined so as to obtain the best description of the experimental data on the static compression, including the melting curve and isotherms, as well as of the results obtained in the shock compression experiments reported in the present study and in Refs. 6–9. The parameters found in this way were as follows: $\rho_k = 1.77$ g/cm^3, $n = 2$; $a_1 = -1057.33$, $a_2 = 3467.23$, $a_3 = -3837.22$, $a_4 = 1427.32$ (a_i all in kilobars); $T_0 = 83.8$ K; $\Theta_0 = 93.3$ K; $\delta_0 = 0.8$; $l = 3$; $r = 1$; $a = 1.7925$; $b = 0.694$; $c = -0.0589$.

The equations of state of the solid and liquid phases were used to calculate the isotherms, melting curve, and shock adiabats. The results are presented in Figs. 3–6 and in Table II. A comparison of the calculated and experimental isotherms[5] and of the melting curves[1–14] shown in Figs. 3 and 4 indicated that they were in satisfactory agreement.

Dynamic compression of argon had been investigated before. The first results were reported by Van Thiel and Alder[8] who determined the shock adiabat from an initial liquid state ($\rho_0 = 1.4$ g/cm^3, $T_0 = 87$ K). Recently Nellis and Mitchell[9] reported shock compression of liquid argon to ~900 kbar. The results of shock compression from the same initial state are reported below. They are compared with the data from Refs. 8 and 9 in Fig. 5. The same figure includes the experimental results from Ref. 26. All these data are in reasonable agreement. The shock adiabat for single compression calculated in the present paper for the initial liquid state ($\rho_0 = 1.4$ g/cm^3) intersects twice the melting curve: at $P = 2$ kbar it enters the solid phase region, at $P = 11$ kbar it reaches a two-phase region (point a in Fig. 4), and at $P = 19$ kbar (point b) it emerges again into the liquid phase.

A comparison of the calculated shock adiabat with the experimental data on single compression shows good agreement only up to pressures of ~300 kbar. At higher pressures the calculated curve is steeper.

Compression by two shock waves was used in Refs. 8 and 10 and one experimental point was obtained in the present study at $\rho = 3.31$ g/cm^3. It is clear from Fig. 5 that a much weaker compression was recorded in Ref. 10 and in our experiments than that reported in Ref. 8. The calculated shock adiabat corresponding to double compression (curve 3 in Fig. 5) was in good agreement with our measurements and with the experiments reported in Ref. 10.

The calculated shock adiabat is compared in Fig. 6 with the experimental results taken from Refs. 6 and 7, which were obtained by compression of solid argon from an initial state $\rho_0 = 1.65$ g/cm^3, $T_0 = 75$ K. Up to $P = 34$ kbar (point c in Fig. 4) the shock adiabat is in the solid phase, whereas

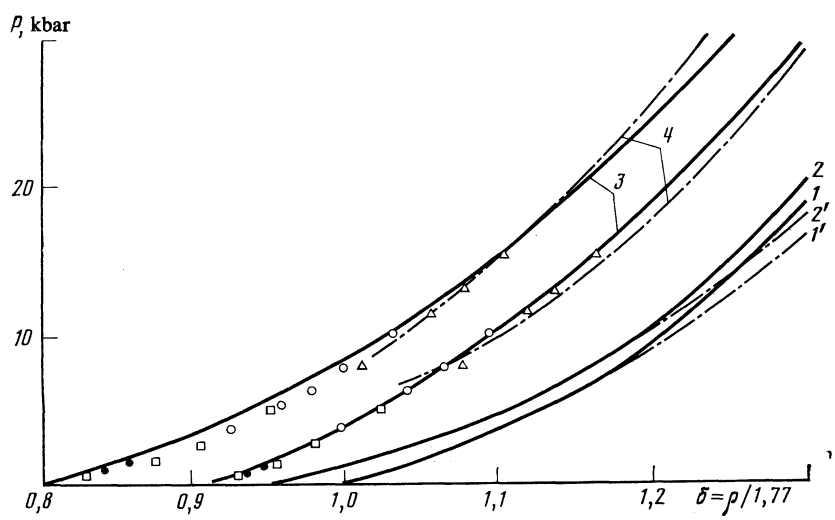

FIG. 3. Comparison of the calculated isotherms of the solid phase and of the melting curve of argon with the experimental results: 1) isotherm at $T = 0$ K (Ref. 5); 2) experimental isotherm at $T = 77$ K (Ref. 5); 1'), 2') isotherms calculated in the present study. Experimental results on the melting curve: ●—from Ref. 11; □—from Ref. 12; ○—from Ref. 13; △—from Ref. 14; 3) melting curve calculated in the present study; 4) melting curve calculated in Ref. 27.

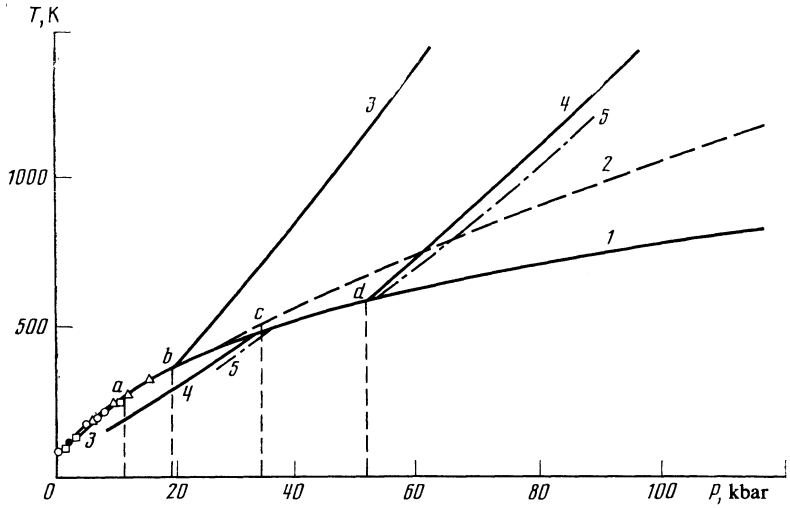

FIG. 4. Melting curve and calculated shock adiabats of argon. Melting curve: ●, □, ○, and △—experimental results from Refs. 11, 12, 13, and 14, respectively; 1) calculation carried out in the present study; 2) calculation taken from Ref. 27. Shock adiabats: 3), 4) calculated in the present study; 5) from Ref. 27 (curve 3 corresponds to the initial liquid state with $\rho_0 = 1.4$ g/cm^3; curves 4 and 5 correspond to the solid state with $\rho_0 = 1.65$ g/cm^3).

$P = 52$ kbar (point d) it enters the liquid pahse, in reasonable agreement with the results of Refs. 6 and 7. The shock adiabats calculated in Ref. 27 differ somewhat from those found in the present study (curves 4 and 5 in Fig. 4). However, the melting curve of Ref. 27 lies somewhat higher.

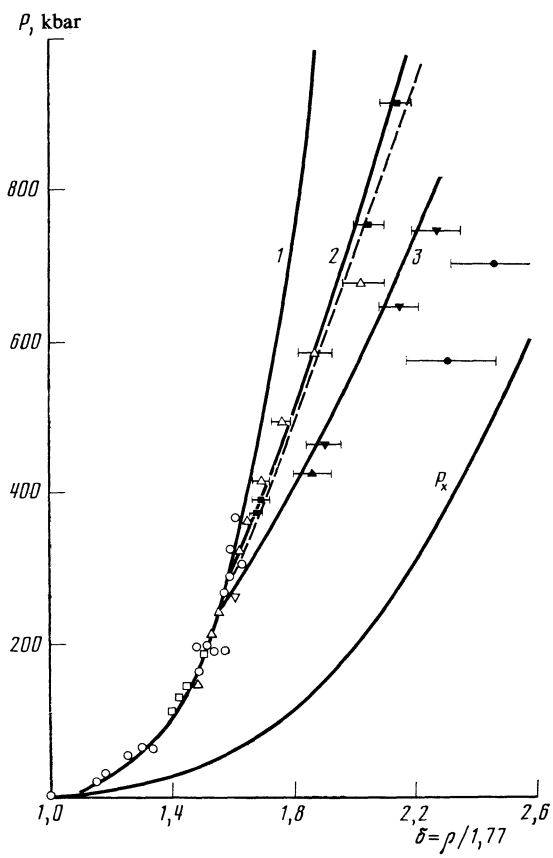

FIG. 5. Shock adiabats of liquid argon. Experimental results: ○ and ●—from Ref. 8; □—from Ref. 26; ▽ and ▼—from Ref. 10; ■—from Ref. 9; △ and ▲—our results. The black circles and triangles correspond to double compression (the horizontal lines crossing the symbols represent the scatter of the experimental data). Calculations: 1) single compression ($\rho_0 = 1.4$ g/cm^3); 2) allowing for electron excitation; 3) double compression; P_x isotherm at $T = 0$; dashed curve taken from Ref. 30.

ROLE OF THERMAL EXCITATION OF ELECTRONS IN SHOCK COMPRESSION OF ARGON

Liquid argon is an insulator at normal pressures and the energy gap between the valence and conduction band in this state is $W \approx 14$ eV. Quantum-mechanical calculations reported in Ref. 28 demonstrate that compression of argon reduces the band gap from $W = 6$ eV at $\rho = 1.9$ g/cm^3 to $W = 2.4$ eV at $\rho = 4.75$ g/cm^3. It is clear from these estimates that, beginning from temperatures of the order of 10^4 K, the contribution of thermal excitation of electrons to the equation of state becomes significant. In the first approximation, this contribution can be allowed for using the theory of

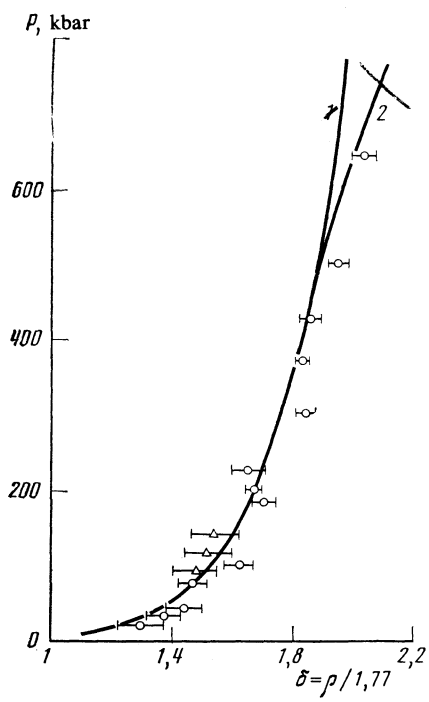

FIG. 6. Shock adiabat of solid argon ($\rho_0 = 1.65$ g/cm^3). Experimental results: ○—from Ref. 6; △—from Ref. 7. Calculations: 1) without allowance for electron excitation; 2) with allowance for electron excitation.

TABLE II.

T, K	P, kbar	δ_L	δ_S	$\Delta S/R$	$\Delta V/V$, %
83,8	0	0,8	0,918	1,74	14,7
170	4,1	0,909	1,002	1,51	10,2
250	9,1	1,009	1,085	1,33	7,5
400	23	1,192	1,246	1,15	4,5
600	55	1,431	1,47	1,06	2,7
800	107	1,661	1,693	1,04	1,9
1200	294	2,105	2,132	1,03	1,3

free electrons, as was done in a description of the experimental shock adiabat of ionic crystals in Ref. 29. By analogy with Ref. 29, we shall describe the electron contribution to the free energy [see Eqs. (1) and (2)] by

$$F_{el}=-\frac{4kT}{\rho}\left(\frac{2\pi m^* kT}{h^2}\right)^{3/2} e^{-W/2kT}, \tag{6}$$

where m^* is the geometric mean of the effective masses of an electron and a hole; k and h are the Boltzmann and Planck constants.

A charge in the density should, in principle, alter both W and m^*, since both these quantities are related to the widths of the energy bands. In our calculations it was assumed, following Ref. 29, that

$$W=W_0\delta^{-\Gamma}, \quad m^*=m_0\delta^{2/3-\Gamma}, \tag{7}$$

where W_0 is the band gap at normal density; m_0 is the mass of a free electron; Γ is an empirical constant the value of which can be found from the condition of the best matching of the shock adiabat at high temperatures. In these calculations we assumed that $W_0 = 14$ eV and $\Gamma = 1$.

The shock adiabat calculated allowing for thermal excitations of electrons is included in Fig. 5 (curve 2). It agrees quite satisfactorily with the experimental data. A dashed curve in Fig. 5 is the calculated shock adiabat of argon taken from Ref. 30, where the dependence of the band gap on the density is assumed to be $W = 12 - 0.14[(22.57/\delta) - 14]^2$ eV. Since curve 2 practically coincides with the dashed curve in Fig. 5, it follows that up to $P \leqslant 1$ Mbar the shock adiabat of argon is not very sensitive to the actual form of the dependence $W(\rho)$.

An allowance for the electron excitation in the case of double compression hardly changes the calculated curve in the investigated region. This is due to the lower temperature behind the front of a reflected shock wave.

COMPARISON OF CALCULATED AND EXPERIMENTAL TEMPERATURES BEHIND THE SHOCK WAVE FRONT

The results of a determination of the brightness temperature of argon are presented in Fig. 7. This figure shows also the experimental results from Ref. 26. Curve 1 is the calculated dependence of the equilibrium temperature obtained by shock compression of liquid argon which—as is clear from the figure—is in satisfactory agreement with the experimental results at pressures up to ~300 kbar. Some increase in the calculated curve in this range may indicate that the equation of state adopted by us describes well the energy and pressure, but underestimates somewhat the specific heat. Beginning from $\sim 10^4$ K, the measured temperature lags considerably behind the calculations. An allowance for electron excitation reduces significantly the calculated temperature on the shock adiabat. This follows from a comparison of curves 1 and 2 in Fig. 7. However, the experimental points lie considerably well below curve 2. This is also true of temperatures determined for alkali halide crystals[31] when, beginning from $T \approx 10^4$ K, there is a systematic lag of the measured temperatures behind those calculated from the equation of state. A semiquantitative theory explaining this effect is proposed in Ref. 32. It is shown there that because of the finite time of the process of transfer of electrons from the valence to the conduction band and their subsequent heating, the "cold" electrons screen the radiation from deeper layers of matter where a temperature equilibrium is established between electrons and the lattice.

We shall give here the main equations that follow from this theory. The time dependences of the densities of electrons and holes are given by

$$\frac{dN}{dt}=g_e N\left[\left(\frac{T}{\theta}\right)^3 e^{-W/kT}-\left(\frac{N}{N_0}\right)^2\right], \tag{8}$$

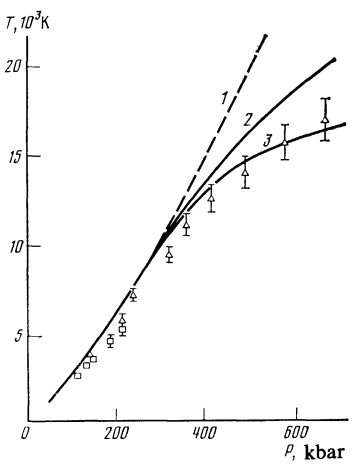

FIG. 7. Calculated and experimental temperatures produced by shock compression of argon ($\rho_0 = 1.4$ g/cm^3). Experimental results: △—our data; □—from Ref. 26 (vertical lines crossing the symbols represent the scatter of the experimental data). Calculations: 1), 2) equilibrium temperature found ignoring and allowing for electron excitation; 3) nonequilibrium temperature found allowing for the electron excitation kinetics.

where θ is the lattice temperature; g_e is a constant describing the electron-electron interaction;

$$N_0=2\left(\frac{2\pi mk\theta}{h^2}\right)^{3/2}.$$

The equation describing the balance of the energies of electrons and holes can be written in the form

$$3kN\frac{dT}{dt}=3kNg_l(\theta-T)-W\frac{dN}{dt}, \qquad (9)$$

where g_l is a constant representing the exchange of energy of the electrons and the lattice. Figure 8 shows the time dependences of the distribution of the electron density in the conduction band and of the electron temperature behind the shock wave front. Initially, there is a brief period during which the electron temperature changes effectively without any change in the electron density. Then, the temperature ceases to vary and the whole energy is used to increase the number of electrons in the conduction band (region I in Fig. 8). When the recombination of electrons with holes begins to play a role comparable with the ionization process creating electrons, the rate of rise of the electron density slows down and the energy acquired by electrons from the lattice is used to increase their temperature and density (region II). This region is interesting because the electron temperature has not yet reached the equilibrium value, but the density of electrons is already high. Since the radiation is emitted from a layer with an optical thickness close to unity, it is possible to determine experimentally the temperature corresponding to the radiation flux from a layer in which the temperature has not reached its equilibrium value.

The radiation flux Φ is

$$\Phi=\int_0^t \Phi_0(T)\alpha\exp\left\{-\int_0^t \alpha\,dl\right\}dl, \qquad (10)$$

where $\Phi_0=(e^{\tau/T}-1)^{-1}$ and $l=(D-u)t$.

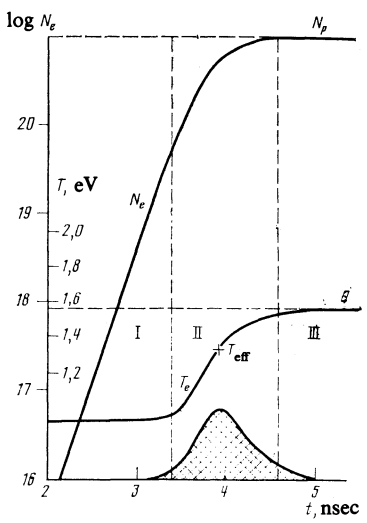

FIG. 8. Dependences of the electron temperature in the conduction band and of the electron density N_e in liquid argon at $\theta=18\,100$ K.

The absorption coefficient α is given by the Drude-Zener relationship

$$\alpha=\frac{2N_ee^2}{ncm^*}\frac{q}{\nu^2+q^2}=1{,}69\cdot10^{-2}\frac{m_0}{m^*}\frac{Nq}{n(\nu^2+q^2)}\ [\mathrm{cm}^{-1}], \qquad (11)$$

where

$$q=1.34\cdot10^{15}\left(\frac{1}{\varepsilon_\infty}-\frac{1}{\varepsilon_0}\right)(T[\mathrm{eV}])^{1/2}\ [\mathrm{sec}^{-1}].$$

Here, the refractive index is $n=[1+\varepsilon_\infty-1)\delta]^{1/2}$, the relative density of the investigated material (argon) is δ, ε_0 and ε_∞ are the static and high-frequency permittivities, and ν is the frequency of the radiation which is being measured.

We used the theory considered in Ref. 32 and summarized briefly above to calculate the brightness temperature of shock-compressed liquid argon. The curve calculated using the parameters $g_l=8\times10^{10}$ sec^{-1} and $g_e=10^{14}$ sec^{-1} is shown in Fig. 7 (curve 3). It is clear from this figure that an allowance for the electron screening ensures a fairly satisfactory agreement with the experimental results. Figure 8 gives the time dependences of the density of free electrons and of their temperature in argon in the case when $\delta=1.9$, $P=590$ kbar, and $\theta=18\,100$ K. At the moment $t=3\times10^{-9}$ sec the electron temperature reaches $T=10\,800$ K and the electron density is $N=3.5\times10^{18}$ cm^{-3}. This rapid rise of the electron density has the effect that a thin layer separated by $\approx4\times10^{-9}$ sec from the leading edge of the front is emitting radiation. The shaded region represents the relative contribution of the various layers inside the shock wave front to the emitted radiation flux. The radiation from deeper layers, where the temperature reaches quite rapidly (in ~1 nsec) its equilibrium value (region III in Fig. 8), is screened by the layers lying ahead and characterized by $T<\theta$. The effective temperature is then 15 500 K.

The results of the present study thus showed that the kinetic theory of the heating of electrons by the lattice phonons proposed in Ref. 32 is valid at least for one more class of condensed substances.

[1]S. B. Kormer, A. I. Funtikov, V. D. Urlin, and A. N. Kolesnikova, Zh. Eksp. Teor. Fiz. **42**, 686 (1962) [Sov. Phys. JETP **15**, 477 (1962)].
[2]S. B. Kormer, M. V. Sinitsyn, G. A. Kirillov, and V. D. Urlin, Zh. Eksp. Teor. Fiz. **48**, 1033 (1965) [Sov. Phys. JETP **21**, 689 (1965)].
[3]V. D. Urlin, Zh. Eksp. Teor. Fiz. **49**, 485 (1965) [Sov. Phys. JETP **22**, 341 (1966)].
[4]F. V. Grigor'ev, S. B. Kormer, O. L. Mikhaĭlova, A. P. Tolochko, and V. D. Urlin, Zh. Eksp. Teor. Fiz. **69**, 743 (1975); **75**, 1683 (1978) [Sov. Phys. JETP **42**, 378 (1975); **48**, 847 (1978)].
[5]J. W. Stewart, J. Phys. Chem. Solids **29**, 641 (1968).
[6]R. D. Dick, R. H. Warnes, and J. Skalyo Jr., J. Chem. Phys. **53**, 1648 (1970).
[7]P. L. Lagus and T. J. Ahrens, J. Chem. Phys. **59**, 3517 (1973).
[8]M. Van Thiel and B. J. Alder, J. Chem. Phys. **44**, 1056 (1966).
[9]W. J. Nellis and A. C. Mitchell, J. Chem. Phys. **73**, 6137 (1980).
[10]W. L. Seitz and J. Wackerle, Bull. Am. Phys. Soc. **17**, 1093 (1972).
[11]W. Van Witzenburg and J. C. Stryland, Can. J. Phys. **46**, 811 (1968).
[12]R. K. Crawford and W. B. Daniels, Phys. Rev. Lett. **21**, 367 (1968).
[13]V. M. Cheng, W. B. Daniels, and R. K. Crawford, Phys. Lett. A **43**, 109 (1973).

[14]S. M. Stishov and V. I. Fedosimov, Pis'ma Zh. Eksp. Teor. Fiz. **14**, 326 (1971) [Sov. Phys. JETP **14**, 217 (1971)].
[15]L. V. Al'tshuler, K. K. Krupnikov, and M. I. Brazhnik, Zh. Eksp. Teor. Fiz. **34**, 886 (1958) [Sov. Phys. JETP **7**, 614 (1958)].
[16]L. V. Al'tshuler, M. N. Pavlovskiĭ, L. V. Kuleshova, and G. V. Simakov, Fiz. Tverd. Tela (Leningrad) **5**, 279 (1963) [Sov. Phys. JETP **5**, 203 (1963)].
[17]L. V. Al'tshuler, A. A. Bakanova, and R. F. Trunin, Zh. Eksp. Teor. Fiz. **42**, 91 (1962) [Sov. Phys. JETP **15**, 65 (1962)].
[18]L. V. Al'tshuler, S. B. Kormer, A. A. Bakanova, and R. F. Trunin, Zh. Eksp. Teor. Fiz. **38**, 790 (1960) [Sov. Phys. JETP **11**, 573 (1960)].
[19]L. V. Al'tshuler, A. A. Bakanova, I. P. Dudoladov, E. A. Dynin, R. F. Trunin, and B. S. Chekin, Zh. Prikl. Mekh. Tekh. Fiz. No. 2, 3 (1981).
[20]L. V. Al'tshuler, Usp. Fiz. Nauk **85**, 197 (1965) [Sov. Phys. Usp. **8**, 52 (1965)].
[21]I. Sh. Model', Zh. Eksp. Teor. Fiz. **32**, 714 (1957) [Sov. Phys. JETP **5**, 589 (1957)].
[22]A. E. Voĭtenko, F. O. Kuznetsov, and I. Sh. Model', Prib. Tekh. Eksp. No. 6, 121 (1962).
[23]S. G. Grenishin, A. A. Solodovnikov, and G. P. Startsev, Tr. Komissii po pirometrii pri VNIIM (Proc. Commission on Pyrometry at All-Union Scientific-Research Institute of Metrology) No. 1, Standartgiz. M., 1958.
[24]S. B. Kormer, Usp. Fiz. Nauk **94**, 641 (1968) [Sov. Phys. Usp. **11**, 229 (1968)].
[25]S. B. Kormer and V. D. Urlin, Dokl. Akad. Nauk SSSR **131**, 542 (1960) [Sov. Phys. Dokl. **5**, 317 (1960)].
[26]I. M. Voskoboinikov, M. F. Gogulya, and Yu. A. Dolgoborodov, Dokl. Akad. Nauk SSSR **246**, 579 (1979) [Sov. Phys. Dokl. **24**, 375 (1979)].
[27]M. Ross, Phys. Rev. A **8**, 1466 (1973).
[28]G. M. Gandel'man, Zh. Eksp. Teor. Fiz. **48**, 758 (1965) [Sov. Phys. JETP **21**, 501 (1965)].
[29]S. B. Kormer, M. V. Sinitsyn, A. I. Funtikov, V. D. Urlin, and A. V. Blinov, Zh. Eksp. Teor. Fiz. **47**, 1202 (1964) [Sov. Phys. JETP **20**, 811 (1965)].
[30]M. Ross, W. Nellis, and A. Mitchell, Chem. Phys. Lett. **68**, 532 (1979).
[31]S. B. Kormer, M. V. Sinitsyn, and A. I. Kuryapin, Zh. Eksp. Teor. Fiz. **55**, 1626 (1968) [Sov. Phys. JETP **28**, 852 (1969)].
[32]Ya. B. Zel'dovich, S. B. Kormer, and V. D. Urlin, Zh. Eksp. Teor. Fiz. **55**, 1631 (1968) [Sov. Phys. JETP **28**, 855 (1969)].

Translated by A. Tybulewicz